PROCEEDINGS OF SCIENCE

Pole Inflation in Supergravity

Constantinos Pallis[a,*]

[a] *Laboratory of Physics, Faculty of Engineering,*
Aristotle University of Thessaloniki,
GR-541 24 Thessaloniki, GREECE

E-mail: kpallis@gen.auth.gr

We show how we can implement, within Supergravity, chaotic inflation in the presence of a pole of order one or two in the kinetic mixing of the inflaton sector. This pole arises due to the selected logarithmic Kahler potentials K, which parameterize hyperbolic manifolds with scalar curvature related to the coefficient $(-N) < 0$ of a logarithmic term. The associated superpotential W exhibits the same R charge with the inflaton-accompanying superfield and includes all the allowed terms. The role of the inflaton can be played by a gauge singlet or non-singlet superfield. Models with one logarithmic term in K for the inflaton, require $N = 2$, some tuning – of the order of 10^{-5} – between the terms of W and predict a tensor-to-scalar ratio r at the level of 0.001. The tuning can be totally eluded for more structured K's, with N values increasing with r and spectral index close or even equal to its present central observational value.

Corfu Summer Institute 2021 "School and Workshops on Elementary Particle Physics and Gravity"
29 August - 9 October 2021
Corfu, Greece

*Speaker

https://pos.sissa.it/

PoS(CORFU2021)078

1. Introduction

Among the many scenarios of inflation, the one which stands out in terms of its simplicity, elegance and phenomenological success is *chaotic inflation* (CI). Most notably, the power-law potentials, employed in models of CI, have the forms

$$V_{\rm I} = \lambda^2\phi^n/n \quad \text{or} \quad V_{\rm I} = \lambda^2(\phi^{n/2} - M^2)^2/n \quad \text{for} \quad M \ll m_{\rm P} = 1, \tag{1}$$

which are very common in physics and so it is easy the identification of the inflaton ϕ with a field already present in the theory. E.g., within *Higgs inflation* (HI) the inflaton could play, at the end of inflation, the role of a Higgs field. However, for $n = 2$ and 4 the theoretically derived values for spectral index $n_{\rm s}$ and/or tensor-to-scalar ratio r are not consistent with the observational ones [1]. A way out of these inconsistencies is to introduce some non-minimality in the gravitational or the kinetic sector of the theory. In this talk, which is based on Refs. [2, 3], we focus on the latter possibility. Namely, our proposal is tied to the introduction of a pole in the kinetic term of the inflaton field. For this reason we call it for short *Pole* (chaotic) *inflation* (PI) [4].

Below we first briefly review the basic ingredients of PI in a non-*Supersymmetric* (SUSY) framework (Sec. 1.1) and constrain the parameters of two typical models in Sec. 1.3 taking into account the observational requirements described in Sec. 1.2. Throughout the text, the subscript $,\chi$ denotes derivation *with respect to* (w.r.t) the field χ, charge conjugation is denoted by a star (*) and we use units where the reduced Planck scale $m_{\rm P} = 2.44 \cdot 10^{18}$ GeV is set equal to unity.

1.1 Non-SUSY Set-up

The lagrangian of the homogenous inflaton field $\phi = \phi(t)$ with a kinetic mixing takes the form

$$\mathcal{L} = \sqrt{-\mathfrak{g}}\left(\frac{N_p}{2f_p^2}\dot\phi^2 - V_{\rm I}(\phi)\right) \quad \text{with} \quad f_p = 1-\phi^p,\ p>0 \ \text{and}\ N_p>0. \tag{2}$$

Also $\mathfrak{g}$ is the determinant of the background Friedmann-Robertson-Walker metric $g^{\mu\nu}$ with signature $(+,-,-,-)$ and dot stands for derivation w.r.t the cosmic time. Concentrating on integer p values we can derive the canonically normalized field, $\widehat\phi$, as follows

$$\frac{d\widehat\phi}{d\phi} = J = \frac{\sqrt{N_p}}{f_p^2} \quad \Rightarrow \quad \widehat\phi = \frac{\sqrt{N_p}}{p}B(\phi^p;1/p,0), \tag{3}$$

where $B(z;m,l)$ represents the incomplete Beta function. Note that $\widehat\phi$ gets increased above unity for $p < 10$ and $0 \leq \phi \lesssim 1$, facilitating, thereby, the attainment of PI with subplanckian ϕ values. Inverting this function we obtain, e.g.,

$$\phi = \begin{cases} 1 - e^{-\widehat\phi/\sqrt{N_1}} & \text{for} \ \ p = 1, \\ \tanh\left(\frac{\widehat\phi}{\sqrt{N_2}}\right) & \text{for} \ \ p = 2\,. \end{cases} \tag{4}$$

As a consequence, Eq. (2) can be brought into the form

$$\mathcal{L} = \sqrt{-\mathfrak{g}}\left(\frac{1}{2}\dot{\widehat\phi}^2 - V_{\rm I}(\phi(\widehat\phi))\right). \tag{5}$$

For $\widehat{\phi} \gg 1$, $V_{\rm I}(\widehat{\phi})$ – expressed in terms of $\widehat{\phi}$ – develops a plateau, and so it becomes suitable for driving inflation of chaotic type called *E-Model Inflation* [5, 6] (or α-Starobinsky model [7]) and *T-Model Inflation* [6, 8] for $p = 1$ and 2 respectively.

1.2 Inflationary Observables – Constraints

The analysis of PI can be performed using the standard slow-roll approximation as analyzed below, together with the relevant observational and theoretical requirements that should be imposed.

(a) The number of e-foldings $N_\star$ that the scale $k_\star = 0.05/{\rm Mpc}$ experiences during PI must be enough for the resolution of the problems of standard Big Bang, i.e., [9]

$$N_\star = \int_{\widehat{\phi}_{\rm f}}^{\widehat{\phi}_*} d\widehat{\phi}\frac{V_{\rm I}}{V_{{\rm I},\widehat{\phi}}} \simeq 61.3 + \frac{1-3w_{\rm rh}}{12(1+w_{\rm rh})}\ln\frac{\pi^2 g_{{\rm rh}*}T_{\rm rh}^4}{30V_{\rm I}(\phi_{\rm f})} + \frac{1}{4}\ln\frac{V_{\rm I}(\phi_\star)^2}{g_{{\rm rh}*}^{1/3}V_{\rm I}(\phi_{\rm f})}, \qquad (6)$$

where $\widehat{\phi}_*$ is the value of $\widehat{\phi}$ when $k_\star$ crosses the inflationary horizon whereas $\widehat{\phi}_{\rm f}$ is the value of $\widehat{\phi}$ at the end of PI, which can be found, in the slow-roll approximation, from the condition

$${\sf max}\{\epsilon(\phi_{\rm f}), |\eta(\phi_{\rm f})|\} = 1, \quad \text{where} \quad \epsilon = \frac{1}{2}\left(\frac{V_{{\rm I},\widehat{\phi}}}{V_{\rm I}}\right)^2 \quad \text{and} \quad \eta = \frac{V_{{\rm I},\widehat{\phi}\widehat{\phi}}}{V_{\rm I}}\,. \qquad (1.7{\sf a})$$

Also we assume that PI is followed in turn by an oscillatory phase with mean equation-of-state parameter $w_{\rm rh}$, radiation and matter domination. We determine it applying the formula [3]

$$w_{\rm rh} = 2\frac{\int_{\phi_{\rm mn}}^{\phi_{\rm mx}} d\phi J(1-V_{\rm I}/V_{\rm I}(\phi_{\rm mx}))^{1/2}}{\int_{\phi_{\rm mn}}^{\phi_{\rm mx}} d\phi J(1-V_{\rm I}/V_{\rm I}(\phi_{\rm mx}))^{-1/2}} - 1, \qquad (1.7{\sf b})$$

where $\phi_{\rm mn} = \langle\phi\rangle$ is the *vacuum expectation value* (v.e.vs) of ϕ after PI. Motivated by implementations [10] of non-thermal leptogenesis, which may follow PI, we set $T_{\rm rh} \simeq 10^9$ GeV for the reheat temperature. Indicative values for the energy-density effective number of degrees of freedom include $g_{{\rm rh}*} = 106.75$ or 228.75 corresponding to the *Standard Model* (SM) or *Minimal SUSY SM* (MSSM) spectrum respectively.

(b) The amplitude $A_{\rm s}$ of the power spectrum of the curvature perturbations generated by ϕ at $k_\star$ has to be consistent with data [9], i.e.,

$$A_{\rm s} = \frac{1}{12\,\pi^2}\frac{V_{\rm I}(\widehat{\phi}_*)^3}{V_{{\rm I},\widehat{\phi}}(\widehat{\phi}_*)^2} \simeq 2.105\cdot 10^{-9}\,. \qquad (8)$$

(c) The remaining inflationary observables ($n_{\rm s}$, its running $\alpha_{\rm s}$ and r) have to be consistent with the latest *Planck release 4* (PR4), *Baryon Acoustic Oscillations* (BAO), CMB-lensing and BICEP/*Keck* (BK18) data [1, 11], i.e.,

$$\text{(i)}\;\; n_{\rm s} = 0.965 \pm 0.009 \quad \text{and} \quad \text{(ii)}\;\; r \leq 0.032, \qquad (9)$$

at 95% *confidence level* (c.l.) – pertaining to the ΛCDM+r framework with $|\alpha_{\rm s}| \ll 0.01$. These observables are estimated through the relations

$$\text{(i)}\;\; n_{\rm s} = 1 - 6\widehat{\epsilon}_\star + 2\widehat{\eta}_\star, \quad \text{(ii)}\;\; \alpha_{\rm s} = \frac{2}{3}\left(4\widehat{\eta}^2 - (n_{\rm s}-1)^2\right) - 2\widehat{\xi}_\star \quad \text{and} \quad \text{(iii)}\;\; r = 16\widehat{\epsilon}_\star\,, \qquad (10)$$

with $\xi = V_{{\rm I},\widehat{\phi}}V_{{\rm I},\widehat{\phi}\widehat{\phi}\widehat{\phi}}/V_{\rm I}^2$ – the variables with subscript $\star$ are evaluated at $\phi = \phi_\star$.

(d) The effective theory describing PI has to remain valid up to a UV cutoff scale $\Lambda_{\rm UV} \simeq m_{\rm P}$ to ensure the stability of our inflationary solutions, i.e.,

$$\text{(i)}\ \ V_{\rm I}(\phi_\star)^{1/4} \leq \Lambda_{\rm UV} \quad \text{and} \quad \text{(ii)}\ \ \phi_\star \leq \Lambda_{\rm UV}. \tag{11}$$

1.3 Results

Using the criteria of Sec. 1.2 we can now analyze the inflationary models based on the potential in Eq. (1) and the kinetic mixing in Eq. (2) for $p = 1$ and 2. The slow-roll parameters are

$$\epsilon = \frac{n^2 f_p}{2N_p\phi^2} \ \text{ and } \ \eta = \frac{nf_p}{N_p\phi^2}\left(n - 1 - (n + p - 1)\phi^p\right), \tag{12}$$

whereas from Eq. (6) we can compute

$$N_\star \simeq \begin{cases} N_1\left(\phi_\star + f_{1\star}\ln f_{1\star}\right)/nf_{1\star} & \text{for } \ p = 1, \\ N_2\phi_\star^2/2nf_{2\star} & \text{for } \ p = 2, \end{cases} \tag{13}$$

where $f_{p\star} = f_p(\phi_\star)$. Since $f_{p\star}$ appears in the denominator, $N_\star$ increases drastically as $\phi_\star$ approaches unity, assuring thereby the achievement of efficient PI. The relevant tuning can be somehow quantified defining the quantity

$$\Delta_\star = 1 - \phi_\star. \tag{14}$$

The naturalness of the attainment of PI increases with $\Delta_\star$. Imposing the condition of Eq. (1.7a) and solving Eq. (13) w.r.t $\phi_\star$, we arrive at

$$\phi_{\rm f} \ll \phi_\star \simeq \begin{cases} nN_\star/(nN_\star + N_1) & \text{for } \ p = 1, \\ \sqrt{2nN_\star/(2nN_\star + N_2)} & \text{for } \ p = 2\,. \end{cases} \tag{15}$$

where we neglect the logarithmic contribution in the first of the relations in Eq. (13). We remark that PI is attained for $\phi < 1$ – and so Eq. (11) is fulfilled – thanks to the location of the pole at $\phi = 1$. On the other hand, Eq. (8) implies

$$\lambda \simeq \left(\sqrt{3nNA_{\rm s}}\pi/N_\star\right)\begin{cases} 2 & \text{for } \ p = 1, \\ 1 & \text{for } \ p = 2\,. \end{cases} \tag{16}$$

From Eq. (10) we obtain the model's predictions

$$n_{\rm s} \simeq 1 - 2/N_\star, \quad \alpha_{\rm s} \simeq -2/N_\star^2 \ \text{ and } \ r \simeq \begin{cases} 8N_1/N_\star^2 & \text{for } \ p = 1, \\ 2N_2/N_\star^2 & \text{for } \ p = 2\,, \end{cases} \tag{17}$$

which are independent of n and for this reason these models are called N-attractors [5–8]. However, the variation of n in Eq. (1) generates a variation to $w_{\rm rh}$ in Eq. (1.7b) and via Eq. (6) to $N_\star$ which slightly distinguish the predictions above. E.g., fixing $N_1 = 10$ we obtain

$$w_{\rm rh} \simeq \begin{cases} -0.08, \\ \ \ 0.19, \end{cases} \quad N_\star \simeq \begin{cases} 49.4, \\ 54.6, \end{cases} \quad \Delta_\star \simeq \begin{cases} 0.074, \\ 0.04, \end{cases} \quad n_{\rm s} \simeq \begin{cases} 0.963 \\ 0.965 \end{cases} \quad r \simeq 0.02 \ \text{ for } \ n = \begin{cases} 2, \\ 4 \end{cases} \tag{1.18a}$$

and $p = 1$ with $\alpha_s \sim 10^{-4}$. Similar α_s values are obtained setting $N_2 = 10$ and $p = 2$ which yields

$$w_{\rm rh} \simeq \begin{cases} -0.04, \\ 0.23, \end{cases} N_\star \simeq \begin{cases} 50.2, \\ 54.6, \end{cases} \Delta_\star \simeq \begin{cases} 0.024, \\ 0.01, \end{cases} n_s \simeq \begin{cases} 0.962, \\ 0.963, \end{cases} r \simeq \begin{cases} 0.0074, \\ 0.0064, \end{cases} \text{for } n = \begin{cases} 2. \\ 4. \end{cases} \tag{1.18b}$$

Notice that $\Delta_\star$ is larger for $p = 1$. Imposing the bound on r in Eq. (9) we can find a robust upper bound on N_p. Namely, we find numerically

$$N_1 \lesssim 19 \ \text{ and } \ N_2 \lesssim 55. \tag{19}$$

Therefore, we can conclude that the presence of f_p in Eq. (2) revitalizes CI rendering it fully consistent with the present data in Eq. (9) without introducing any complication with the validity of the effective theory. Recall [12] that the last problem plagues models of CI with large non-minimal coupling to gravity for $n > 2$.

1.4 Outline

It would be certainly interesting to inquire if it is possible to realize similar models of PI in a SUSY framework where a lot of the problems of SM are addressed. We below describe how we can formulate PI in the context of *Supergravity* (SUGRA) in Sec. 2 and we specify six models of PI: three models (δCI, CI2, CI4) employing a gauge singlet inflaton in Sec. 3 and three (δHI, HI4, HI8) with a gauge non-singlet inflaton in Sec. 4.

2. Realization of PI Within SUGRA

We start our investigation presenting the basic formulation of scalar theory within SUGRA in Sec. 2.1 and then – in Sec. 2.2 – we outline our strategy in constructing viable models of PI.

2.1 General Set-up

The part of the SUGRA lagrangian including the (complex) scalar fields Z^α can be written as

$$\mathcal{L} = \sqrt{-\mathfrak{g}}\left(K_{\alpha\bar\beta} D_\mu Z^\alpha D^\mu Z^{*\bar\beta} - V\right), \tag{2.20a}$$

where the kinetic mixing is controlled by the Kähler potential K and the relevant metric defined as

$$K_{\alpha\bar\beta} = K_{,Z^\alpha Z^{*\bar\beta}} > 0 \ \text{ with } \ K^{\bar\beta\alpha} K_{\alpha\bar\gamma} = \delta^{\bar\beta}_{\bar\gamma}. \tag{2.20b}$$

Also, the covariant derivatives for the scalar fields Z^α are given by

$$D_\mu Z^\alpha = \partial_\mu Z^\alpha + ig A^{\rm a}_\mu T^{\rm a}_{\alpha\beta} Z^\beta \tag{2.20c}$$

with $A^{\rm a}_\mu$ being the vector gauge fields, g the (unified) gauge coupling constant and $T^{\rm a}$ with ${\rm a} = 1, ..., {\rm dim}G_{\rm GUT}$ the generators of a gauge group $G_{\rm GUT}$. Here and henceforth, the scalar components of the various superfields are denoted by the same superfield symbol.

The SUGRA scalar potential, $V_{\rm SUGRA}$, is given in terms of K, and the superpotential, W, by

$$V_{\rm SUGRA} = V_{\rm F} + V_{\rm D} \ \text{ with } \ V_{\rm F} = e^K\left(K^{\alpha\bar\beta} {\rm F}_\alpha {\rm F}^*_{\bar\beta} - 3|W|^2\right) \ \text{ and } \ V_{\rm D} = g^2 \sum_{\rm a} {\rm D}_{\rm a}{\rm D}_{\rm a}/2, \tag{2.20d}$$

where a trivial gauge kinetic function is adopted whereas the F- and D-terms read

$$\mathrm{F}_\alpha = W_{,Z^\alpha} + K_{,Z^\alpha} W \quad \text{and} \quad \mathrm{D}_\mathrm{a} = Z_\alpha \, (T_\mathrm{a})^\alpha_\beta \, K^\beta \quad \text{with} \quad K^\alpha = K_{,Z^\alpha} \,. \tag{2.20e}$$

Therefore the models of PI in Sec. 1.1 can be supersymmetrized, if we select conveniently the functions K and W so that Eqs. (1) and (2) are reproduced.

2.2 Modeling PI in SUGRA

We concentrate on PI driven by V_F. To achieve this, we have to assure that $V_\mathrm{D} = 0$ during PI. This condition may be attained in the following two cases:

- If the inflaton is (the radial part of) a gauge singlet superfield $Z^2 := \Phi$. In this case, Φ has obviously zero contribution to V_D.
- If the inflaton is the radial part of a conjugate pair of Higgs superfields, $Z^2 := \Phi$ and $Z^3 := \bar\Phi$, which are parameterized so as $V_\mathrm{D} = 0$ – see Sec. 4.

The achievement of a kinetic term in Eq. (2.20a) similar to that in Eq. (2) for $p = 1$ and 2 we need to establish suitable K's so that

$$\langle K\rangle_\mathrm{I} = -N \ln f_p \quad \text{and} \quad \langle K_{\alpha\bar\beta}\rangle_\mathrm{I} = N/f_p \tag{21}$$

with N related to N_p. However, from the F-term contribution to Eq. (2.20d), we remark that K affects besides the kinetic mixing V_SUGRA, which, in turn, depends on the W too. Therefore, f_p is generically expected to emerge also in the denominator of V_SUGRA making difficult the establishment of an inflationary era. This problem can be surpassed [2, 3] by two alternative strategies:

- Adjusting W and constraining the prefactor of K's, so that the pole is removed from V_SUGRA thanks to cancellations [2, 3, 15] which introduce some tuning, though.
- Adopting a structured K which yields the desired kinetic terms in Eq. (2) but remains invisible from V_SUGRA [2, 3, 16]. In a such case, any tuning on the W parameters can be eluded

In Sec. 3 and 4 we show details on the realization of these scenaria taking into account that f_1 in Eq. (2) can be exclusively associated with a gauge singlet inflaton whereas f_2 can be related to a gauge non-singlet inflaton.

We reserved $\alpha = 1$ for a gauge singlet superfield, $Z^1 = S$ called stabilizer or goldstino, which assists [13] us to formulate PI of chaotic type in SUGRA. Its presence in W is determined as follows:

- It appears linearly in W multiplying its other terms. To achieve technically such a adjustment we require that S and W are equally charged under an R symmetry.
- It generates for $\langle S\rangle_\mathrm{I} = 0$ the inflationary potential via the only term of V_SUGRA which remains alive

  $$V_\mathrm{I} = \langle V_\mathrm{F}\rangle_\mathrm{I} = \langle e^K K^{SS^*} |W_{,S}|^2\rangle_\mathrm{I}, \tag{22}$$

  where the symbol "$\langle Q\rangle_\mathrm{I}$" denotes the value of a quantity Q during PI.

- It assures the boundedness of $V_{\rm I}$. Indeed, if we set $\langle S\rangle_{\rm I}=0$, then $\langle K_{,z^\alpha}W\rangle_{\rm I}=0$ for $\alpha\neq 1$ and $-3|\langle W\rangle_{\rm I}|^2=0$. Obviously, non-vanishing values of the latter term may render $V_{\rm F}$ unbounded from below.

- It can be stabilized at $\langle S\rangle_{\rm I}=0$ without invoking higher order terms, if we select [14]

$$K_2=N_S\ln\left(1+|S|^2/N_S\right)\quad\Rightarrow\quad\langle K_2^{SS^*}\rangle_{\rm I}=1\ \text{ with } 0<N_S<6. \tag{23}$$

  K_2 parameterizes the compact manifold $SU(2)/U(1)$. Note that for $\langle S\rangle_{\rm I}=0$, S is canonically normalized and so we do not mention it again henceforth.

3. PI With a Gauge Singlet Inflaton

The SUGRA setup for this case is presented in Sec. 3.1 and then – in Sec. 3.2 – we describe the salient features of this model and we expose our results in Sec. 3.3.

3.1 SUGRA Set-up

This setting is realized in presence of two gauge singlet superfields S and Φ. We adopt the most general renormalizable W consistent with the R symmetry mentioned in Sec. 2.2, i.e.,

$$W=S\left(\lambda_1\Phi+\lambda_2\Phi^2-M^2\right) \tag{24}$$

where λ_1,λ_2 and M are free parameters. As regards K, this includes besides K_2 in Eq. (23) one of the following K's, $K_{1\rm s}$ or $\widetilde K_{1\rm s}$, which yield a pole of order one in the kinetic term of Φ and share the same geometry – see Ref. [3]. Namely,

$$K_{1\rm s}=-N\ln\left(1-(\Phi+\Phi^*)/2\right)\quad\text{or}\quad\widetilde K_{1\rm s}=-N\ln\frac{(1-\Phi/2-\Phi^*/2)}{(1-\Phi)^{1/2}(1-\Phi^*)^{1/2}}, \tag{25}$$

with $\mathsf{Re}(\Phi)<1$ and $N>0$. We opt a pole of order one as the simplest choice although models with a pole of order two were also proposed [5]. Based on the K's above, we can define the following three versions of PI:

- δCI, where the total K is chosen as

$$K_{21\rm s}=K_2+K_{1\rm s}. \tag{3.26a}$$

  The elimination of pole in $V_{\rm I}$ discussed above can be applied if we set

$$N=2\quad\text{and}\quad r_{21}=-\lambda_2/\lambda_1\simeq 1+\delta_{21}\quad\text{with}\quad\delta_{21}\sim 0\quad\text{and}\quad M\ll 1 \tag{3.26b}$$

  such that the denominator including the pole in $V_{\rm I}$ is (almost) cancelled out.

- CI2 and CI4, which do not display any denominator in $V_{\rm I}$ employing

$$\widetilde K_{21\rm s}=K_2+\widetilde K_{1\rm s} \tag{27}$$

  with free parameters N,λ_1,λ_2 and M. The discrimination of these models depends on which of the two ϕ-dependent terms in Eq. (24) dominates – see below.

3.2 Structure of the Inflationary Potential

An inflationary potential of the type in Eq. (1) can be derived from Eq. (22) specifying the inflationary trajectory as follows

$$\langle S\rangle_{\rm I}=0 \quad\text{and}\quad \langle\theta\rangle_{\rm I}:=\arg\langle\Phi\rangle_{\rm I}=0. \tag{28}$$

Inserting the quantities above into Eq. (22) and taking into account Eq. (23) and

$$\langle e^K\rangle_{\rm I}=\begin{cases} f_1^{-N} & \text{for}\quad K=K_{21{\rm s}},\\ 1 & \text{for}\quad K=\widetilde{K}_{21{\rm s}},\end{cases} \tag{29}$$

we arrive at the following master equation

$$V_{\rm I}=\lambda^2\begin{cases}\left(\phi-r_{21}\phi^2-M_1^2\right)^2/f_1^N & \text{for } \delta{\sf CI},\\ \left(\phi-r_{21}\phi^2-M_1^2\right)^2 & \text{for } {\sf CI2},\\ \left(\phi^2-r_{12}\phi-M_2^2\right)^2 & \text{for } {\sf CI4},\end{cases} \tag{30}$$

where $\phi={\rm Re}(\Phi)$, $r_{ij}=-\lambda_i/\lambda_j$ with $i,j=1,2$ and λ and M_i are identified as follows

$$\lambda=\begin{cases}\lambda_1 \ \text{and}\ M_1=M/\sqrt{\lambda_1} & \text{for } \delta{\sf CI} \text{ and } {\sf CI2},\\ \lambda_2 \ \text{and}\ M_2=M/\sqrt{\lambda_2} & \text{for } {\sf CI4}.\end{cases} \tag{31}$$

As advertised in Sec. 3.1, the pole in f_1 is presumably present in $V_{\rm I}$ of δCI, but it disappears for CI2 and CI4. The arrangement of Eq. (3.26b), though, renders the pole harmless for δCI.

The correct description of PI is feasible if we introduce the canonically normalized fields, $\widehat{\phi}$ and $\widehat{\theta}$ as follows

$$\langle K_{\Phi\Phi^*}\rangle_{\rm I}|\dot{\Phi}|^2\simeq\frac{1}{2}\left(\dot{\widehat{\phi}}^2+\dot{\widehat{\theta}}^2\right)\ \Rightarrow\ \frac{d\widehat{\phi}}{d\phi}=J=\frac{\sqrt{N/2}}{f_1}\ \text{and}\ \widehat{\theta}\simeq J\phi\theta\ \text{with}\ \langle K_{\Phi\Phi^*}\rangle_{\rm I}=\frac{N}{4f_1^2}. \tag{32}$$

We see that the relation between ϕ and $\widehat{\phi}$ is identical with Eq. (3) for $p=1$, if we do the replacement $N_1=N/2$. We expect that CI2 [CI4] yield similar results with the non-SUSY models of PI with $p=1$ in Eq. (2) and $n=2$ [$n=4$] in Eq. (1), whereas δCI is totally autonomous.

To check the stability of $V_{\rm SUGRA}$ in Eq. (2.20d) along the trajectory in Eq. (28) w.r.t the fluctuations of Z^α's, we construct the mass spectrum of the theory. Our results are summarized in Table 1. Taking into the limit $\delta_{21}=M_1=0$ for δCI, $r_{21}=M_1=0$ for CI2 and $r_{12}=M_2=0$ for CI4, we find the expressions of the masses squared $\widehat{m}^2_{\chi^\alpha}$ (with $\chi^\alpha=\theta$ and s) arranged in Table 1. We there display the masses $\widehat{m}^2_{\psi^\pm}$ of the corresponding fermions too – we define $\widehat{\psi}_\Phi=J\psi_\Phi$ where ψ_Φ and ψ_S are the Weyl spinors associated with S and Φ respectively. We notice that the relevant expressions can take a unified form for all models – recall that we use $N=2$ in δCI – and approach, close to $\phi=\phi_\star\simeq1$, rather well the quite lengthy, exact ones employed in our numerical computation. From them we can appreciate the role of $N_S<6$ in retaining positive $\widehat{m}^2_s$. Also, we confirm that $\widehat{m}^2_{\chi^\alpha}\gg H_{\rm I}^2\simeq V_{\rm I0}/3$ for $\phi_{\rm f}\leq\phi\leq\phi_\star$.

FIELDS	EIGEN-STATES	MASSES SQUARED		
			$K = K_{21\mathrm{s}}$	$K = \widetilde{K}_{21\mathrm{s}}$
1 real scalar	$\widehat{\theta}$	$\widehat{m}^2_\theta$	$6H_\mathrm{I}^2$	
2 real scalars	$\widehat{s}_1,\ \widehat{s}_2$	$\widehat{m}^2_s$	$6H_\mathrm{I}^2/N_S$	
2 Weyl spinors	$(\widehat{\psi}_\Phi \pm \widehat{\psi}_S)/\sqrt{2}$	$\widehat{m}^2_{\psi\pm}$	$6n(1-\phi)^2H_\mathrm{I}^2/N\phi^2$	

Table 1: *Mass spectrum of our CI models along the inflationary trajectory of Eq.* (3.5) *– we take $n = 1$ for δCI and CI2 whereas $n = 2$ for CI4.*

3.3 Results

The dynamics of the analyzed models is analytically studied in Ref. [3]. We here focus on the numerical results. After imposing Eqs. (6) and (8) the free parameters of

$$\delta\mathsf{CI},\ \mathsf{CI2},\ \mathsf{CI4}\quad \text{are}\quad (\delta_{21}, M_1), (N, r_{21}, M_1)\ \text{ and }\ (N, r_{12}, M_2),$$

respectively. Recall that we use $N = 2$ exclusively for δCI. Fixing $M_1 = 0.001$ for δCI, $M_1 = 0.01$ and $r_{21} = 0.001$ for CI2 and $M_2 = 0.01$ and $r_{12} = 0.001$ for CI4, we obtain the curves plotted and compared to the observational data in Fig. 1. We observe that:

(a) For δCI the resulting n_s and r increase with $|\delta_{21}|$ – see solid line in Fig. 1. This increase, though, is more drastic for n_s which covers the whole allowed range in Eq. (9). From the considered data we collect the results

$$0 \lesssim \delta_{21}/10^{-6} \lesssim 3.3 \quad 3.5 \lesssim r/10^{-3} \lesssim 5.3 \quad \text{and} \quad 9\cdot 10^{-3} \lesssim \Delta_\star \lesssim 0.01. \tag{33}$$

In all cases we obtain $N_\star \simeq 44$ consistently with Eq. (6) and the resulting $w_\mathrm{rh} \simeq -0.237$ from Eq. (1.7b). Fixing $n_\mathrm{s} = 0.965$ we find $\delta_{21} = -1.7\cdot 10^{-5}$ and $r = 0.0044$ – see the leftmost column of the Table in Fig. 1.

(b) For CI2 and CI4, n_s and r increase with N and $\Delta_\star$ which increases w.r.t its value in δCI. Namely, n_s approaches its central observational value in Eq. (9) whereas the bound on r yields an upper bound on N. More quantitatively, for CI2 – see dashed line in Fig. 1 – we obtain

$$0.96 \lesssim n_\mathrm{s} \lesssim 0.9654,\ \ 0.1 \lesssim N \lesssim 65,\ \ 0.05 \lesssim \Delta_\star/10^{-2} \lesssim 16.7\ \text{ and }\ 0.0025 \lesssim r \lesssim 0.039 \tag{3.34a}$$

with $w_\mathrm{rh} \simeq -0.05$ and $N_\star \simeq 50$. On the other hand, for CI4 – see dot-dashed line in Fig. 1 – we obtain

$$0.963 \lesssim n_\mathrm{s} \lesssim 0.965,\ \ 0.1 \lesssim N \lesssim 55,\ \ 0.23 \lesssim \Delta_\star/10^{-2} \lesssim 8.5\ \text{ and }\ 0.0001 \lesssim r \lesssim 0.04 \tag{3.34b}$$

with $w_\mathrm{rh} \simeq (0.25 - 0.39)$ and $N_\star \simeq 54 - 56$. In both equations above the lower bound on N is just artificial. For $N = 10$, specific values of parameters and observables are arranged in the rightmost columns of the Table in Fig. 1.

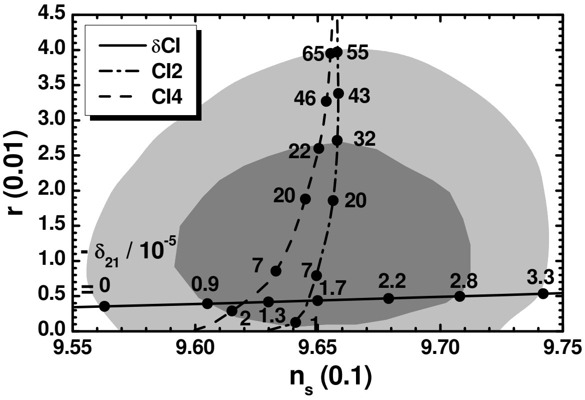

Model:	δCI	CI2	CI4
δ_{21} / r_{21} / r_{12}	$-1.7\cdot10^{-5}$	0.001	0.001
N	2	10	10
$\phi_\star/0.1$	9.9	9.53	9.84
$\Delta_\star(\%)$	1	4.7	2
$\phi_{\rm f}/0.1$	6.66	3.7	5.6
$w_{\rm rh}$	−0.24	−0.08	0.26
$N_\star$	44.4	51.5	55.5
$\lambda/10^{-5}$	1.2	2.1	1.9
$n_{\rm s}/0.1$	9.65	9.64	9.65
$-\alpha_{\rm s}/10^{-4}$	11.4	6.7	6.2
$r/10^{-2}$	0.44	1.3	1.1

Figure 1: *Allowed curves in the $n_{\rm s}-r$ plane for (i) δCI, $M_1=0.01$ and various δ_{21}'s indicated on the solid line or (ii) CI2, $M_1=0.01$ and $r_{21}=0.001$ or CI4, $M_2=0.01$ and $r_{12}=0.001$ and various N's indicated on the dashed or dot-dashed line respectively. The marginalized joint 68% [95%] c.l. regions [11] from PR4, BK18, BAO and lensing data-sets are depicted by the dark [light] shaded contours. The relevant field values, parameters and observables corresponding to points shown in the plot are listed in the Table.*

4. PI With a Gauge non-Singlet Inflaton

In the present scheme the inflaton field can be identified with the radial component of a conjugate pair of Higgs superfields. We here focus on the Higgs superfields, $\bar\Phi$ and Φ, with $B-L=-1,\ 1$ which break the GUT symmetry $G_{\rm GUT}=G_{\rm SM}\times U(1)_{B-L}$ down to SM gauge group $G_{\rm SM}$ through their v.e.vs. We below outline the SUGRA setting in Sec. 4.1 its inflationary outcome in Sec. 4.2) and its predictions in Sec. 4.3. We here update the results of Ref. [2], taking into account the recent data of Ref. [11], and enrich its content adding the model HI8.

4.1 SUGRA Set-up

In accordance with the imposed symmetries, we here adopt the following W – cf. Ref. [17]:

$$W=S\left(\frac{1}{2}\lambda_2\bar\Phi\Phi+\lambda_4(\bar\Phi\Phi)^2-\frac{1}{4}M^2\right),\tag{35}$$

where λ_2,λ_4 and M are free parameters. In contrast to Eq. (24), we here include the first allowed non-renormalizable term to activate the pole-elimination method – see below. On the other hand, the invariance of K under $G_{\rm GUT}$ enforces us to introduce a pole of order two within the kinetic terms of $\bar\Phi-\Phi$ system. One possible option – for another equivalent one see Ref. [2] – is

$$K_{21}=-N\ln\left(1-|\Phi|^2-|\bar\Phi|^2\right)\quad\text{or}\quad\widetilde K_{21}=-N\ln\frac{1-|\Phi|^2-|\bar\Phi|^2}{(1-2\bar\Phi\Phi)^{1/2}(1-2\bar\Phi^*\Phi^*)^{1/2}},\tag{36}$$

which parameterizes the manifold $\mathcal{M}_{21}=SU(2,1)/(SU(2)\times U(1))$ [2] – note that the present N is twice that defined in the first paper of Ref. [2]. From the selected above W and K's, the following inflationary models emerge:

- δHI, where we employ

$$K_{221}=K_2+K_{21}\tag{4.37a}$$

and ensure an elimination of the singular denominator appearing in $V_{\rm I}$ setting

$$N=2\quad\text{and}\quad r_{42}=-\lambda_4/\lambda_2\simeq 1+\delta_{42}\quad\text{with}\quad \delta_{42}\sim 0\quad\text{and}\quad M\ll 1. \tag{4.37b}$$

- HI4 and HI8, which do not display any singularity in $V_{\rm I}$, employing

$$\widetilde{K}_{221}=K_2+\widetilde{K}_{21} \tag{38}$$

with free parameters N, λ_2, λ_4 and M. Their discrimination depends on which of the two ϕ-dependent terms in Eq. (35) dominates – see below.

4.2 Structure of the Inflationary Potential

As in Sec. 3.2, we determine the inflationary potential, $V_{\rm I}$, selecting a suitable parameterization of the involved superfields. In particular, we set

$$\Phi=\phi e^{i\theta}\cos\theta_\Phi\quad\text{and}\quad \bar\Phi=\phi e^{i\bar\theta}\sin\theta_\Phi\quad\text{with}\quad 0\leq\theta_\Phi\leq\pi/2\quad\text{and}\quad S=(s+i\bar{s})/\sqrt{2}. \tag{39}$$

We can easily verify that a D-flat direction is

$$\langle\theta\rangle_{\rm I}=\langle\bar\theta\rangle_{\rm I}=0,\ \langle\theta_\Phi\rangle_{\rm I}=\pi/4\quad\text{and}\quad\langle S\rangle_{\rm I}=0, \tag{40}$$

which can be qualified as inflationary path. Indeed, for both K's in Eq. (27), the D term due to $B-L$ symmetry during PI is

$$\langle {\rm D}_{BL}\rangle_{\rm I}=N\left(|\langle\Phi\rangle_{\rm I}|^2-|\langle\bar\Phi\rangle_{\rm I}|^2\right)/\left(1-|\langle\Phi\rangle_{\rm I}|^2-|\langle\bar\Phi\rangle_{\rm I}|^2\right)=0. \tag{41}$$

Also, regarding the exponential prefactor of $V_{\rm F}$ in Eq. (2.20d) we obtain

$$\langle e^K\rangle_{\rm I}=\begin{cases} f_2^{-N} & \text{for}\quad K=K_{21},\\ 1 & \text{for}\quad K=\widetilde{K}_{21},\end{cases} \tag{42}$$

Substituting it and Eqs. (23) and (35) into Eq. (22), this takes its master form

$$V_{\rm I}=\frac{\lambda^2}{16}\begin{cases}\left(\phi^2-r_{42}\phi^4-M_2^2\right)^2/f_2^N & \text{for }\delta\text{HI},\\ \left(\phi^2-r_{42}\phi^4-M_2^2\right)^2 & \text{for HI4},\\ \left(\phi^4-r_{24}\phi^2-M_4^2\right)^2 & \text{for HI8},\end{cases} \tag{43}$$

where $r_{ij}=-\lambda_i/\lambda_j$ with $i,j=1,2$ and λ and M_i are identified as follows

$$\lambda=\begin{cases}\lambda_2\quad\text{and}\quad M_2=M/\sqrt{\lambda_2} & \text{for }\delta\text{HI and HI4},\\ \lambda_4\quad\text{and}\quad M_4=M/\sqrt{\lambda_4} & \text{for HI8}.\end{cases} \tag{44}$$

From Eq. (43), we infer that the pole in f_2 is presumably present in $V_{\rm I}$ of δHI but it disappears in $V_{\rm I}$ of HI4 and HI8and so no N dependence in $V_{\rm I}$ arises. The elimination of the pole in the regime of Eq. (4.37b) lets open the realization of δHI, though.

FIELDS	EIGEN-STATES	MASSES SQUARED		
			$K=K_{221}$	$K=\widetilde{K}_{221}$
2 real scalars	$\widehat{\theta}_+$	$m^2_{\widehat{\theta}+}$	$3H_{\rm I}^2$	
	$\widehat{\theta}_\Phi$	$\widehat{m}^2_{\theta_\Phi}$	$M_{BL}^2+6H_{\rm I}^2(1+2/N-2/N\phi^2)$	
1 complex scalar	$s,\bar{s}$	$\widehat{m}^2_s$	$6H_{\rm I}^2(1/N_S-8(1-\phi^2)/N+N\phi^2/2$ $+2(1-2\phi^2)+8\phi^2/N)$	$6H_{\rm I}^2(1/N_S-4/N$ $+2/N\phi^2+2\phi^2/N)$
1 gauge boson	A_{BL}	M_{BL}^2	$2Ng^2\phi^2/f_2^2$	
4 Weyl spinors	$\widehat{\psi}_\pm$	$\widehat{m}^2_{\psi\pm}$	$12f_2^2H_{\rm I}^2/N^2\phi^2$	
	$\lambda_{BL},\widehat{\psi}_{\Phi-}$	M_{BL}^2	$2Ng^2\phi^2/f_2^2$	

Table 2: *Mass spectrum the models of HI along the inflationary trajectory of Eq.* (4.8).

To obtain PI we have to correctly identify the canonically normalized (hatted) fields of the $\bar{\Phi}-\Phi$ system, defined as follows

$$\langle K_{\alpha\bar\beta}\rangle_{\rm I}\dot{Z}^\alpha\dot{Z}^{*\bar\beta}\simeq\frac{1}{2}\left(\dot{\widehat{\phi}}^2+\dot{\widehat{\theta}}_+^2+\dot{\widehat{\theta}}_-^2+\dot{\widehat{\theta}}_\Phi^2\right)\quad\text{for}\quad\alpha=2,3. \tag{4.45a}$$

– recall that $Z^1=S$ is already canonically normalized for $\langle S\rangle_{\rm I}=0$ as in Eq. (40). We find

$$\left(\langle K_{\alpha\bar\beta}\rangle_{\rm I}\right)=\langle M_{\Phi\bar\Phi}\rangle_{\rm I}\ \text{with}\ \langle M_{\Phi\bar\Phi}\rangle_{\rm I}=\frac{\kappa\phi^2}{2}\begin{pmatrix}2/\phi^2-1 & 1\\ 1 & 2/\phi^2-1\end{pmatrix},\ \kappa=\frac{N}{f_2^2}. \tag{4.45b}$$

We then diagonalize $\langle M_{\Phi\bar\Phi}\rangle_{\rm I}$ via a similarity transformation, i.e.,

$$U_{\Phi\bar\Phi}\langle M_{\Phi\bar\Phi}\rangle_{\rm I}U_{\Phi\bar\Phi}^{\sf T}=\mathrm{diag}\,(\kappa_+,\kappa_-)\,,\quad\text{where}\quad U_{\Phi\bar\Phi}=\frac{1}{\sqrt2}\begin{pmatrix}1&1\\-1&1\end{pmatrix},\ \kappa_+=\kappa\ \text{ and }\ \kappa_-=\kappa f_2\,. \tag{46}$$

Inserting the expressions above in Eq. (4.45a) we obtain the hatted fields

$$\frac{d\widehat\phi}{d\phi}=J=\frac{\sqrt{2N}}{f_2},\ \ \widehat\theta_+\simeq\sqrt{\kappa_+}\phi\theta_+,\ \ \widehat\theta_-\simeq\sqrt{\kappa_-}\phi\theta_-\ \text{ and }\ \widehat\theta_\Phi\simeq\phi\sqrt{2\kappa_-}\,(\theta_\Phi-\pi/4)\,, \tag{47}$$

where $\theta_\pm=\left(\bar\theta\pm\theta\right)/\sqrt2$. From the first equation above we conclude that Eq. (3) for $p=2$ is reproduced for $N_2=2N$. We expect that δHI has similar behavior with δCI, found in Sec. 3.2 whereas HI4 [HI8] may be interpreted as supersymmetrization of the non-SUSY models with $p=2$ in Eq. (2) and $n=4$ [$n=8$] in Eq. (1).

Having defined the canonically normalized scalar fields, we can derive the mass spectrum of our models along the direction of Eq. (40) and verify its stability against the fluctuations of the non-inflaton fields. Approximate, quite precise though, expressions for $\phi=\phi_\star\sim1$ are arranged in Table 2. We confine ourselves to the limits $\delta_{42}=M_2=0$ for δHI, $r_{42}=M_2=0$ for HI4 and $r_{24}=M_4=0$ for HI8. As in the case of the spectrum in Table 1, $N_S<6$ plays a crucial role in retaining positive and heavy enough $\widehat{m}_s^2$. Here, however, we also display the masses, M_{BL}, of the gauge boson A_{BL} (which signals the fact that $U(1)_{B-L}$ is broken during PI) and the masses of the corresponding fermions. The unspecified eigenstate $\widehat{\psi}_\pm$ is defined as

$$\widehat{\psi}_\pm = (\widehat{\psi}_{\Phi+} \pm \psi_S)/\sqrt{2} \quad \text{where} \quad \psi_{\Phi\pm} = (\psi_\Phi \pm \psi_{\bar{\Phi}})/\sqrt{2}\,, \tag{48}$$

with the spinors ψ_S and $\psi_{\Phi\pm}$ being associated with the superfields S and $\bar{\Phi} - \Phi$. It is also evident that A_{BL} becomes massive absorbing the massless Goldstone boson associated with $\widehat{\theta}_-$.

The breakdown of $U(1)_{B-L}$ during PI is crucial in order to avoid the production of topological defects during the $B - L$ phase transition, which takes place after end of PI. Indeed, along the direction of Eq. (40), $V_{\rm I}$ develops a SUSY vacuum lying at the direction

$$\langle S\rangle = 0 \quad \text{and} \quad \langle\phi\rangle = \begin{cases} \left(1-(1-4r_{42}M_2^2)^{1/2}\right)^{1/2}/\sqrt{2r_{42}} & \text{for } \delta\text{HI and HI4,} \\ \left(r_{24}+(r_{24}^2+4M_4^2)^{1/2}\right)^{1/2}/\sqrt{2} & \text{for HI8,} \end{cases} \tag{49}$$

i.e., $U(1)_{B-L}$ is finally spontaneously broken via the v.e.v of ϕ.

4.3 Results

As in Sec. 3.3 we here focus on our numerical results – our analytic ones for δHI and HI4 are presented in Ref. [2]. After enforcing Eqs. (6) and (8) – which yield λ together with $\phi_\star$ – the free parameters of the models

$$\delta\text{HI},\ \text{HI4},\ \text{HI8} \quad \text{are} \quad (\delta_{42}, M_2), (N, r_{42}, M_2) \ \text{and} \ (N, r_{24}, M_4),$$

respectively. Recall that we use $N = 2$ exclusively for δHI. Also, we determine M_2 and M_4 demanding that the GUT scale within MSSM $M_{\rm GUT} \simeq 2/2.433\times10^{-2}$ is identified with the value of M_{BL} – see Table 2 – at the vacuum of Eq. (49), I.e.,

$$\langle M_{BL}\rangle = \frac{\sqrt{2N}g\langle\phi\rangle}{\langle f_p\rangle} = M_{\rm GUT} \ \Rightarrow\ \langle\phi\rangle \simeq \frac{M_{\rm GUT}}{g\sqrt{2N}} \ \text{with} \ g\simeq 0.7,\ \langle f_p\rangle \simeq 1 \tag{50}$$

and $\langle\phi\rangle$ given by Eq. (49). By varying the remaining parameters for each model we obtain the allowed curves in the $n_{\rm s} - r$ plane– see Fig. 2. A comparison with the observational data is also displayed there. We observe that:

(a) For δHI – see the solid line in Fig. 2 – we obtain results similar to those obtained for δCI in Sec. 3.3. Namely, the resulting $n_{\rm s}$ and r increase with $|\delta_{42}|$ with $n_{\rm s}$ covering the whole allowed range in Eq. (9). From the considered data we collect the results

$$2 \lesssim -\delta_{42}/10^{-5} \lesssim 5.5, \quad 2 \lesssim r/10^{-3} \lesssim 3.6 \quad \text{and} \quad 4 \lesssim \Delta_\star/10^{-3} \lesssim 4.75. \tag{51}$$

Also we obtain $N_\star \simeq (54.8 - 55.7)$ consistently with Eq. (6) and the resulting $w_{\rm rh} \simeq 0.3$ from Eq. (1.7b). Fixing $n_{\rm s} = 0.965$ we find $\delta_{42} = -3.6\cdot10^{-5}$ and $r = 0.0026$ – see the leftmost column of the Table in Fig. 2. Eq. (50) gives $M_2 = 0.00587$.

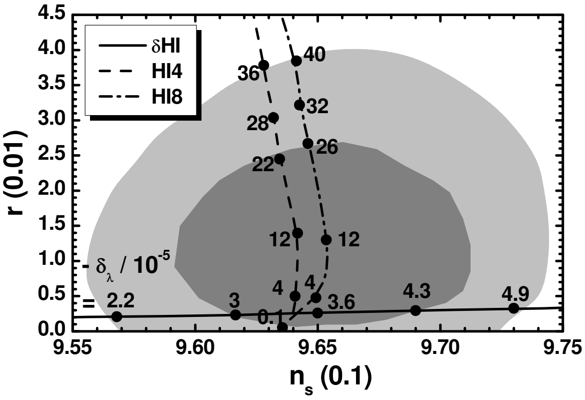

Model:	δHI	HI4	HI8
δ_{42} / r_{42} / r_{24}	$-3.6\cdot10^{-5}$	0.01	10^{-6}
N	2	12	12
$\phi_\star/0.1$	9.9555	9.75	9.877
$\Delta_\star(\%)$	0.445	2.5	1.23
$\phi_{\rm f}/0.1$	5.9	3.9	6.5
$w_{\rm rh}$	0.33	0.266	0.58
$N_\star$	55.2	56.4	58
$\lambda/10^{-5}$	3.6	8.6	8.5
$n_{\rm s}/0.1$	9.65	9.64	9.65
$-\alpha_{\rm s}/10^{-4}$	6.6	6.4	5.98
$r/10^{-2}$	0.26	1.4	1.3

Figure 2: *Allowed curves in the $n_{\rm s}-r$ plane fixing $M_{BL}=M_{\rm GUT}$ for (i) δHI and various δ_{42}'s indicated on the solid line or (ii) HI4 and $r_{42}=0.01$ or HI8 and $r_{24}=10^{-6}$ and various N's indicated on the dashed and dot-dashed line respectively. The shaded corridors are identified as in Fig. 1. The relevant field values, parameters and observables corresponding to points shown in the plot are listed in the Table.*

(b) For HI4 and HI8, $n_{\rm s}$ and r increase with N and $\Delta_\star$ which is larger than this obtained in δHI. Namely, $n_{\rm s}$ approaches its central observational value in Eq. (9) whereas the bound on r yields an upper bound on N. More specifically, for HI4 – see dashed line in Fig. 2 – we obtain

$$0.963 \lesssim n_{\rm s} \lesssim 0.964,\quad 0.1 \lesssim N \lesssim 36,\quad 0.09 \lesssim \Delta_\star/10^{-2} \lesssim 7.6\ \text{ and }\ 0.0005 \lesssim r \lesssim 0.039\,, \quad (4.52a)$$

with $w_{\rm rh}\simeq0.3$ and $N_\star\simeq56$. Eq. (50) dictates $M_2\simeq(0.0013-0.0045)$. On the other hand, for HI8 – see dot-dashed line in Fig. 2 – we obtain

$$0.963 \lesssim n_{\rm s} \lesssim 0.965,\quad 0.1 \lesssim N \lesssim 40,\quad 0.45 \lesssim \Delta_\star/10^{-2} \lesssim 3.8\ \text{ and }\ 0.0001 \lesssim r \lesssim 0.039\,, \quad (4.52b)$$

with $w_{\rm rh}\simeq(0.25-0.6)$ and $N_\star\simeq(54.6-60)$. Eq. (50) implies $M_4\simeq(1.1-690)\cdot10^{-6}$. In both equations above the lower bound on N is just artificial – as in Eqs. (3.34a) and (3.34b). For $N=12$, specific values of parameters and observables are arranged in the rightmost columns of the Table in Fig. 2. Although HI8 is worse than HI4 regarding the tuning of M_4 and r_{24}, it leads to $n_{\rm s}$ values precisely equal to its central observational one – cf. Eq. (9).

5. Conclusions

We reviewed the implementation of PI first in a non-SUSY and then to a SUSY framework. In the former regime, we confined ourselves to models displaying a kinetic mixing in the inflaton sector with a pole of order one or two and verified their agreement with observations. In the latter regime, we presented two classes of models (CI and HI) depending on whether the inflaton is included into a gauge singlet or non-singlet field. CI and HI are relied on the superpotential in Eqs. (24) and (35) respectively which respects an R symmetry and include an inflaton accompanying field which facilitates the establishment of PI. In each class of models we singled out three subclasses of models (δCI, CI2 and CI4) and (δHI, HI4 and HI8). The models δCI and δHI are based on Kähler potentials in Eqs. (3.26a) and (4.37a) whereas (CI2, CI4) and (HI4, HI8) in those shown in Eqs. (27) and (38). All those Kähler potentials parameterize hyperbolic internal geometries with a kinetic pole of order one for CI and two for HI. The Higgflaton in the last case implements the breaking of a gauge $U(1)_{B-L}$ symmetry at a scale which may assume a value compatible with the MSSM unification.

All the models excellently match the observations by restricting the free parameters to reasonably ample regions of values. In particular, within δCI and δHI any observationally acceptable n_s is attainable by tuning δ_{21} and δ_{42} respectively to values of the order 10^{-5}, whereas r is kept at the level of 10^{-3} – see Eqs. (33) and (51). On the other hand, CI2, CI4, HI4 and HI8 avoid any tuning, larger r's are achievable as N increases beyond 2, while n_s lies close to its central observational value – see Eqs. (3.34a) and (3.34b) for CI and Eqs. (4.52a) and (4.52b) for HI.

Acknowledgments This research work was supported by the Hellenic Foundation for Research and Innovation (H.F.R.I.) under the "First Call for H.F.R.I. Research Projects to support Faculty members and Researchers and the procurement of high-cost research equipment grant" (Project Number: 2251).

References

[1] Y. Akrami *et al.* [*Planck* Collaboration], *Planck 2018 results. X. Constraints on inflation*, *Astron. Astrophys.* **641**, A10 (2020) [arXiv:1807.06211].

[2] C. Pallis, *Pole-Induced Higgs Inflation With Hyperbolic Kaehler Geometries*, *JCAP* **05**, 043 (2021) [arXiv:2103.05534]; C. Pallis, *$SU(2,1)/(SU(2)\times U(1))$ B-L Higgs Inflation*, *J. Phys. Conf. Ser.* **2105**, no. 12, 12 (2021) [arXiv:2109.06618].

[3] C. Pallis, *An Alternative Framework for E-Model Inflation in Supergravity*, arXiv:2204.01047.

[4] B.J. Broy, M. Galante, D. Roest and A. Westphal, *Pole inflation, Shift symmetry and universal corrections*, *JHEP* **12**, 149 (2015) [arXiv:1507.02277]; T. Terada, *Generalized Pole Inflation: Hilltop, Natural, and Chaotic Inflationary Attractors*, *Phys. Lett. B* **760**, 674 (2016) [arXiv:1602.07867].

[5] R. Kallosh, A. Linde, and D. Roest, *Superconformal Inflationary a-Attractors*, *JHEP* **11**, 198 (2013) [arXiv:1311.0472].

[6] R. Kallosh and A. Linde, *BICEP/Keck and cosmological attractors*, *JCAP* **12**, no. 12, 008 (2021) [arXiv:2110.10902].

[7] J. Ellis, M.A. G. Garcia, D.V. Nanopoulos, K.A. Olive and S. Verner, *BICEP/Keck constraints on attractor models of inflation and reheating*, *Phys. Rev. D* **105**, no. 4, 043504 (2022) [arXiv:2112.04466].

[8] R. Kallosh and A. Linde, *Universality Class in Conformal Inflation*, *JCAP* **07**, 002 (2013) [arXiv:1306.5220].

[9] N. Aghanim *et al.* [*Planck* Collaboration], *Planck 2018 results. VI. Cosmological parameters*, *Astron. Astrophys.* **641**, A6 (2020) – Erratum: *Astron. Astrophys.* **652**, C4 (2021) [arXiv:1807.06209].

[10] C. Pallis and N. Toumbas, *Non-Minimal Higgs Inflation and non-Thermal Leptogenesis in a Supersymmetric Pati-Salam Model*, *JCAP* **12**, 002 (2011) [arXiv:1108.1771]; C. Pallis, *Gravitational Waves, μ Term & Leptogenesis from $B-L$ Higgs Inflation in Supergravity*, *Universe* **4**, no. 1, 13 (2018) [arXiv:1710.05759].

[11] M. Tristram *et al.*, *Improved limits on the tensor-to-scalar ratio using BICEP and Planck*, *Phys. Rev. Lett.* **127**, 151301 (2021) [arXiv:2112.07961].

[12] C. Pallis, *Models of Non-Minimal Chaotic Inflation in Supergravity*, *PoS* **Corfu2012**, 061 (2013) [arXiv:1307.7815].

[13] R. Kallosh, A. Linde and T. Rube, *General inflaton potentials in supergravity, Phys. Rev. D* **83**, 043507 (2011) [arXiv:1011.5945].

[14] C. Pallis and N. Toumbas, *Starobinsky-Type Inflation With Products of Kähler Manifolds*, *JCAP* **05**, no. 05, 015 (2016) [arXiv:1512.05657]; C. Pallis and N. Toumbas, *Starobinsky Inflation: From Non-SUSY To SUGRA Realizations*, *Adv. High Energy Phys.* **2017**, 6759267 (2017) [arXiv:1612.09202].

[15] J. Ellis, D.V. Nanopoulos and K.A. Olive, *No-Scale Supergravity Realization of the Starobinsky Model of Inflation*, *Phys. Rev. Lett.* **111**, 111301 (2013) – Erratum: *Phys. Rev. Lett.* **111**, no. 12, 129902 (2013) [arXiv:1305.1247].

[16] J.J.M. Carrasco, R. Kallosh, A. Linde and D. Roest, *Hyperbolic geometry of cosmological attractors*, *Phys. Rev. D* **92**, no. 4, 041301 (2015) [arXiv:1504.05557].

[17] R. Jeannerot, S. Khalil, G. Lazarides and Q. Shafi, *Inflation and Monopoles in Supersymmetric* $SU(4)_{\rm c}\times SU(2)_L\times SU(2)_R$, *JHEP* **10**, 012 (2000) [hep-ph/0002151].